Current and Future Test Reference Years at a 5 km Resolution

C Liu*, W Chung, F Cecinati, S Natarajan and D Coley

Department of Architecture and Civil Engineering, University of Bath, Claverton Down, Bath, BA2 7AY, UK

Abstract

Frequently, the computer modelling of the natural and human-made environment requires localised weather files. Traditionally, the weather files are based on the observed weather at a small number of locations (14 for the UK). Unfortunately, both the climate and the weather are known to be highly variable across the landscape, so the small number of locations has the potential to cause large errors. With respect to buildings, this results in incorrect estimates of the annual energy use (sometimes by a factor of 2), or of overheating risk. Here we use a validated weather generator running on a 5x5 km grid to create probabilistic Test Reference Years (pTRYs) for the UK at 11,326 locations. We then investigate the spatial variability of these pTRYs and of annual energy estimates and temperatures in buildings generated by them, both now and in 2080. Further pTRYs targeted at understanding the impact of minimum and maximum temperatures are proposed and produced at the same locations. Finally, we place these pTRYs, which represent the first set of reference weather files at this spatial resolution in the world and that include the urban heat island effect, into a publicly accessible database so researchers and industry can access them.

Practical applications:

Insufficiently localised weather data for building simulations has limited the accuracy of previous estimations of energy use and overheating risk in buildings. This work produces localised probabilistic Test Reference Years (pTRYs) across the whole UK for now and future climates. In addition, a new pTRY method has been proposed in order to overcome an unexpected shortcoming of traditional pTRYs in representing typical maximum and minimum temperatures. These current and future weather data will be of interest to various disciplines including those interested in low carbon design, renewable energy and climate resilience.

Keywords

Spatial variability, climate change, weather files, built environment

***Corresponding author:**
C Liu, University of Bath, Claverton Down, Bath, BA2 7AY, UK
E-mail address: C.Liu2@bath.ac.uk

1. Introduction

Global warming due to anthropogenic emissions has the potential for a series of adverse effects on human health, the built environment, agriculture and other systems. Thanks in part to the computer simulation of the future climate, some of these impacts have been studied. For instance, the risk of overheating, heat-related deaths and energy consumption in buildings[1-15]. These studies rely on high fidelity predictions of future weather, and such predictions are of equal importance to those interested in renewable energy productivity, crop yields, etc. today and under changing climate. Though there are uncertainties in any predictions due to limitations in modelling techniques and an imperfect understanding of the climate system, modelling with future climates is likely to be increasingly beneficial in studying climate related problems and avoiding climate related disasters, and hence in discussing resilience and creating policy. However in all cases there is the need for the underlying weather files to accurately reflect the variability of the climate across the landscape and include the impact of the urban environment on the temperature time series [1, 5, 16]. Hence, *localised* reference weather years are required.

Unfortunately, current and future weather years are unavailable at a high spatial resolution for any country. In the UK, for instance, the Chartered Institution of Building Services Engineers (CIBSE) provides Test Reference Years (TRYs) and Design Summer Years (DSYs) for use in building simulation only for fourteen UK sites, with for example the whole of Scotland being covered by only two files: one sited in Edinburgh and the other in Glasgow; and all buildings in Wales, even in upland areas, modelled as if they are located in coastal Cardiff. The reason for the small number of sites is largely due to the limited availability of reliable and long-term observed weather time series.

The CIBSE TRYs were created for use in evaluation of building energy performance while the CIBSE DSYs were created for use in assessment of overheating risk and cooling loads. Levermore and Parkinson (2006) [17] proposed methods for creating the CIBSE TRYs and DSYs based on around 21 years of historical weather data collected between 1983 and 2005. Eames *et al.* (2015) [18] updated these CIBSE TRYs and DSYs based on around 30 years of observed weather data available until 2013. In addition, Eames *et al.* (2011) [19] created future probabilistic TRYs (pTRYs) and DSYs (pDSYs) using future synthetic weather data generated by the UKCP09 Weather Generator (WG) [20, 21]. CIBSE released these future weather files for fourteen UK sites too. As demonstrated in Eames *et al.* (2012)'s [5] work for instance, fourteen sites are insufficient for accurate predictions of internal climate and energy use. Even the expansion to 45 locations through the PROMETHEUS project [19] is too few to investigate spatial variation in, for instance, energy demand, or the morbidity or mortality from overheating in the homes of the vulnerable. Satellite remote sensing datasets could be used for identifying spatial variation in land surface temperature (e.g. urban heat or cool island effect). However, it has been challenging to retrieve and validate satellite-derived land surface temperatures [22]. Moreover, it has been hard to derive all the thermally related hourly weather variables from satellite remote sensing datasets that are required in the creation of building simulation weather files.

In this work we use a validated weather generator driven by the outputs of a climate model to produce, for the first time, reference weather years on a 5x5 km grid across the UK, thereby giving examples of current and future weather at 11,326 locations. We then investigate the spatial variability of this weather and of the resultant expected annual energy use and temperatures in buildings, both now and in 2080.

2. Creation of pTRYs using the Spatial Urban Weather Generator

2.1. Synthetic weather data

The UKCP09 Weather Generator (WG) provides current and future synthetic weather data which have been used for creating building simulation weather files in previous studies [4, 19, 23-27]. The UKCP09 WG is a stochastic tool that primarily generates the precipitation sequence based on the Neyman-Scott Rectangular Pulses model [28]. Then, the precipitation sequence is used to produce the time series of the other weather variables based on inter-variable relationships observed from the baseline climate data over the control period (1961 to 1990).

In this study, the Spatial Urban Weather Generator (SUWG)[29], an updated version of the UKCP09 WG with improved capability to generate extreme weather and spatially correlated climate, was used to generate climate data for the whole of the UK. The SUWG generates daily weather variables for the control period in order to fit these to the observed statistics. Hourly weather variables are then downscaled from daily weather variables. Each run of the SUWG also generates future synthetic weather data which incorporate an estimate of climate change randomly sampled from 10,000 UKCP09 probabilistic climate change projections. The probabilistic climate change projections were formed by regional and global climate models, i.e., multi-model ensembles [20].

Unlike the UKCP09 WG, the SUWG also takes account of the impacts of land use (i.e. the urban fraction) and anthropogenic heat flux on the temperature time series, by making use of the urban anthropogenic components developed by McCarthy *et al.* (2012) [30]. This means that the urban heat island (UHI) effect can be explored.

A comparison of the outputs of the SUWG and the UKCP09 WG is presented in Table 1. Key differences are:

- the UKCP09 WG can generate future weather data for seven future time slices under three emission scenarios, while the SUWG only produces these for five future time slices (the 2020s, 2030s, 2040s, 2050s and 2080s) under the medium emission scenario (SRES A1B).
- the UKCP09 WG does not provide wind speed directly, so the FAO Penman-Monteith equation [31] for estimating the potential evapotranspiration ($mm \cdot day^{-1}$) needed to be rearranged to calculate the daily wind speed [19]. The SUWG, on the other hand, includes wind speed. Then hourly wind direction can be obtained by using the method proposed by Eames *et al.* (2011) [19]. A complete set of weather variables required for the creation of EnergyPlus Weather (EPW) files, which have been commonly used in various dynamic building simulation packages such as EnergyPlus, DesignBuilder, IES<VE> and ESP-r, can be derived from the outputs of the SUWG using the method presented in previous works [27, 32-34].

Table 1. Comparison between the Spatial Urban Weather Generator (SUWG) and the UKCP09 Weather Generator (WG)

		SUWG	UKCP09 WG
Emission scenarios	Low (SRES B1)		✓
	Medium (SRES A1B)	✓	✓
	High (SRES A1FI)		✓
Time slices	Control year (1970s): 1961 - 1990	✓	✓
	2020s: 2010 - 2039	✓	✓
	2030s: 2020 - 2049	✓	✓
	2040s: 2030 - 2059	✓	✓
	2050s: 2040 - 2069	✓	✓
	2060s: 2050 - 2079		✓
	2070s: 2060 - 2089		✓
	2080s: 2070 - 2099	✓	✓
Output variables			
Daily data	1. Mean total daily precipitation (mm)	✓	✓
	2. Minimum daily temperature (°C)	✓	✓
	3. Maximum daily temperature (°C)	✓	✓
	4. Vapour pressure (hPa)	✓	✓
	5. Relative humidity (%)	✓	✓
	6. Wind speed ($m \cdot s^{-1}$)	✓	
	7. Sunshine hours (hr)	✓	✓
	8. Diffuse irradiation ($kWh \cdot m^{-2}$)	✓	✓
	9. Direct irradiation ($kWh \cdot m^{-2}$)	✓	✓
	10. Potential evapotranspiration ($mm \cdot day^{-1}$)	✓	✓
Hourly data	1. Mean total hourly precipitation rate (mm)	✓	✓
	2. Mean hourly temperature (°C)	✓	✓
	3. Vapour pressure (hPa)	✓	✓
	4. Relative humidity (%)	✓	✓
	5. Wind speed ($m \cdot s^{-1}$)	✓	
	6. Sunshine hours (hr)	✓	✓
	7. Direct irradiation ($Wh \cdot m^{-2}$)	✓	✓
	8. Diffuse irradiation ($Wh \cdot m^{-2}$)	✓	✓

2.2. Creation of pTRYs based on the synthetic weather data from the SUWG

As the SUWG can provide spatially correlated current and future climate data, it has been possible to explore the spatial variability of external temperatures under changing climate. The SUWG was used to create building simulation weather files at 11,326 grid locations. To avoid bias in projected estimates, the SUWG was run 100 times per grid location by incorporating 100 estimates of randomly sampled probabilistic climate change projections into the control period, i.e., 1961 to 1990. Therefore, 100 sets of 30-year long control year (1970s) and future climate (for the 2080s under medium emission scenario) data were generated at the same time for each grid location. The method proposed by Eames *et al.* (2011) [19] was deployed to produce probabilistic Test Reference Years (pTRYs) for the 11,326 locations. With such a high resolution climate data, it has become possible to investigate influence of spatial variability of climate on buildings across the UK. As an example of the result, high-resolution maps of the mean external temperature of the pTRYs as well as the mean internal temperature generated by them for the 2080s (2070 to 2099) are presented in Figure 3.

3. Reference building

In order to explore the influence of the spatial variability of current and future climate on energy and thermal performance of buildings, dynamic thermal simulation for all 11,326 grid locations was carried out. As the idea was only to provide an example, a single building morphology was used: a south facing detached house - a typical UK dwelling architype. This was modelled using DesignBuilder (version 5.0.3.007)[35]. Figure A-1 (see Append) shows the geometry, floor plan and glazing dimension of the building, which was based on the detached house found in BEPAC Technical Note 90/2 [36] but with slightly modified dimensions to be in line with the latest English Housing Survey [37] at the time of writing this paper.

Shading was included by assuming that east and west sides of the house were shaded by adjacent houses with the same building height while there was no shading to the rear of the house (i.e. north). Based on the Residential Design Guide [38], the distance between the adjacent houses was set to 2 m which is the minimum requirement for side access to rear gardens while the privacy distance between facing houses (i.e. to the south) was set to 27.5 m (see Figure A-2 in Append). The U-values suggested by RdSAP 2012 version 9.93 [39] were used, see Table A-1 and Table A-2 in Append.

DesignBuilder uses EnergyPlus[40] as its simulation engine which provides two ventilation options: scheduled and calculated. The scheduled ventilation option was used in this study as it is less computer intensive and hence has a lower time burden, which was an advantage when simulating at 11,326 locations. As the airtightness of existing UK dwellings has not been improved significantly over the past decades [41, 42], the background air infiltration rate was set to 0.7 ac/h in accordance with BRECSU[43]'s recommendation. This value was also suggested by Allen and Pinney (1990) for creating a thermal model of standard UK dwellings. The effective air change rates for conventional two-story residential buildings were obtained from the Standard Assessment Procedure (SAP version 9.92) [44]. The recommended maximum effective air change rates when the house is naturally ventilated during summer are presented in Table A-3, while occupancy, equipment and lighting profiles are shown in Table A-4 (see Append). The number of occupants was assumed to be the number of bedrooms plus one, with the occupancy profile for a working couple with two children. Regarding natural ventilation during the cooling season (April to September), windows were assumed to be open during occupied hours when internal temperature exceeded 22°C, which is in line with the window opening rule used in CIBSE TM36 [45, 46] as well as previous modelling based UK overheating studies [3, 47-49]. During the heating season (October to March) radiators were turned on and off based on the heating set-point temperature of 20°C between 5 p.m. and 9 a.m.

The annual gas use for space heating predicted from the thermal model of the reference house was 124.6 kWh·m^{-2} for London (i.e. Gatwick Airport, 51°09' N, 0°) under the current climate. This is close to the UK household energy consumption for space heating (125.0 kWh·m^{-2})[50]. The annual electricity use of the reference building (floor area of 110 m^2) was 4365 kWh which is also close to the electricity consumption of real detached houses with similar floor area (i.e. 4400 kWh for floor area between 101 m^2 and 150 m^2) [51] in the UK.

Table 2 presents indoor mean and maximum temperatures predicted from the thermal model of the reference house and those found from UK national survey on summertime overheating in 193 English homes [52]. The indoor temperatures were monitored (08:00-22:00 for living rooms while 23:00-07:00 for bedrooms between 22nd July and 31st August in 2007) across nine UK government office regions including North East, West Midlands, Yorkshire, South West, East Midlands, North West, East of England, South East and London [52]. Due to the lack of localised weather data for the same monitoring period, the current CIBSE TRYs for the same regions were used in this study to examine whether or

not summertime temperatures of the reference house were representative. As shown in Table 2, the external mean and maximum temperatures averaged over the nine regions for the monitored period between 22nd July and 31st August in 2007, i.e., $\overline{T_{ex}^{mean}}$ and $\overline{T_{ex}^{max}}$ were 15.3°C and 27.0°C respectively. The monitored period was found to be the coolest summer between 1998 and 2007 [52]. Also, the monitored period was cooler than the CIBSE TRYs as evidenced by the fact that the mean and maximum temperatures of the CIBSE TRYs averaged over the same regions were 16.7°C and 28.2°C respectively. As can be seen in Table 2, the predictions (i.e., $\overline{T_{in}^{mean}}$ and $\overline{T_{in}^{max}}$) are slightly warmer than the monitored values, most likely because the survey was conducted during the cool summer of 2007, however they are very close and hence the thermal model of the reference house can be considered as reasonably representative.

Table 2. Comparison between the monitored data [52] and predictions from the thermal model. Note all the values shown in this table were averaged over the nine UK government office regions: North East, West Midlands, Yorkshire, South West, East Midlands, North West, East of England, South East and London. ±values are standard deviations.

Indoor	**Monitored data from UK national survey**		**Predictions from the thermal model of the reference house in this study**	
	Living room	Bedroom	Living room	Bedroom
$\overline{T_{in}^{mean}}$ (°C)	21.8 ±0.4	21.6 ±0.5	22.6 ±0.6	21.2 ±0.6
$\overline{T_{in}^{max}}$ (°C)	25.7 ±1.0	25.4 ±0.8	27.8 ±1.6	25.6 ±1.0
Outdoor	**Measured data from UK national survey**		**Current CIBSE TRYs [53]**	
$\overline{T_{ex}^{mean}}$ (°C)	15.3 ±1.0		16.7 ±0.8	
$\overline{T_{ex}^{max}}$ (°C)	27.0*		28.2 ±1.7	

*Standard deviation of the external maximum temperatures was unavailable from the reference [52]

4. Spatial variability of the probabilistic Test Reference Years

As mentioned in the introduction, it is well known that the annual heating energy use and summertime temperatures of UK homes vary across the landscape, especially in areas with large topographic differences [1, 5]. As presented in Figure 1, the UK landscape indeed shows great topographic variation, and hence we would expect any TRY data set with high spatial resolution to show similar variation. In this section we examine the spatial variation in the mean external temperature of pTRY (T_{ex}^{mean}) and the mean summertime internal temperature ($T_{in,s}^{mean}$) and gas use for heating (kWh·m^{-2} per year) for the reference house.

4.1. Adjusting external temperatures by using the environmental lapse rate

In Figure 1, map A shows the spatial variability of the surface altitude at a 5 km by 5 km grid resolution across the UK landscape. The altitude datasets were derived from the Global Land One-km Base Elevation Project database [54]. The database was aggregated to the same 5 km grid of the synthetic weather data generated by the SUWG for the UK. Map B shows the expected resultant spatial variation in temperature caused by this altitude, given by the environmental lapse rate (–0.6°C/100m). Map C shows the 14 CIBSE weather regions and the annual mean external temperature (T_{ex}^{mean}) as found in each CIBSE TRY. Comparing the map A and map C it is clear that 14 CIBSE TRYs are not sufficient to represent localised weather. Most commercial thermal modelling software allows the weather file to be adjusted for altitude by using the environmental lapse rate although it is unknown if most researchers or engineers do so. Map D in Figure 1 illustrates the impact of simply adjusting for altitude in this way. Although, much detail is added, artefacts can still be observed, such as the spatial discontinuity in the south east, again suggesting localised weather is needed.

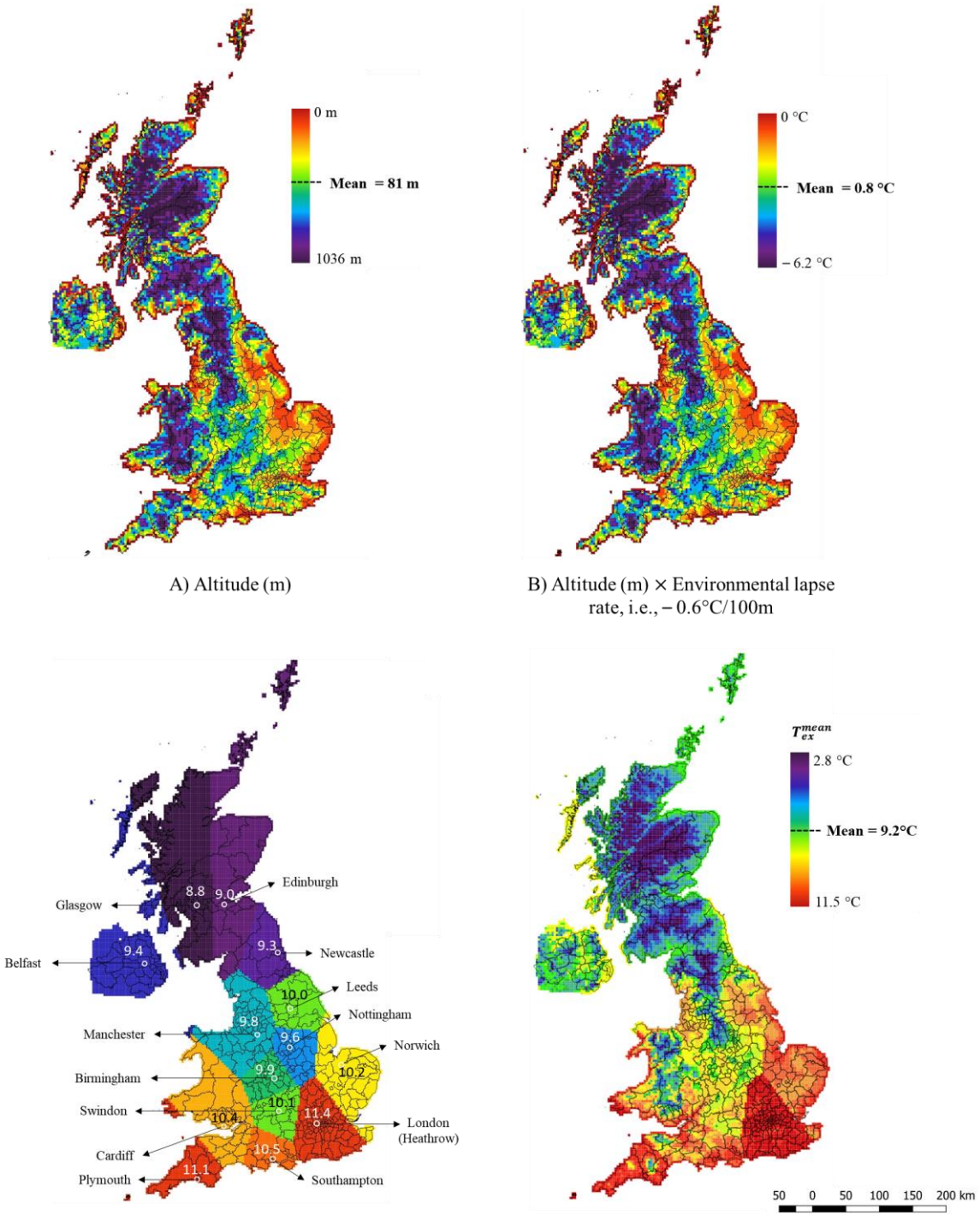

Figure 1. A) Spatial variability of surface altitude of the UK at a 5 km resolution; B) expected decrease in hourly temperatures through the application of an environmental lapse rate of −0.6°C per 100m of altitude; C) the regions covered by the 14 current TRYs together with their annual mean temperatures; D) the effect of applying an environmental lapse rate of −0.6°C per 100m of altitude on current CIBSE TRYs. Quantile map classification was used, except for map C, so that each class contained approximately the same number of grids.

4.2. Spatial variability of external and internal mean temperatures

Spatial variations in external (T_{ex}^{mean}) and internal summertime mean temperatures ($T_{in,s}^{mean}$) across the UK are presented in Figure 3. Summer is defined as April to September for the reference building. No heating was used during this period. The largest cities in the UK are marked and the urban heat island effect is clearly noticeable. For instance, T_{ex}^{mean} and $T_{in,s}^{mean}$ for urban areas such as London, Birmingham and Manchester are respectively on average 1.5°C and 1.0°C warmer than rural areas.

A classic technique for measuring spatial continuity is through a semivariogram (see Figure 2), i.e., an observation plot showing change in variability over increasing separation distances [55]. A semivariogram uses semivariance ($\gamma(h)$), which is a measure of spatial dependence of the values of attribute Z between two points on a surface, $Z(x)$ and $Z(x+h)$ with a separation defined by the lag, h [56]:

$$\gamma(h) = \frac{1}{2N(h)} \sum_{i=1}^{N(h)} [Z(x_i) - Z(x_i + h)]^2 \quad (1)$$

where $N(h)$ is the number of data pairs that are approximately separated by lag, h. The distance where the semivariogram first flattens out (after which semivariance does not increase anymore) is termed the *range*, and the semivariance value at this point, the absolute *sill*. The *nugget*, which describes the variability at distances tending to zero, represents both small scale variability inherent in the studied process and measurement errors. It can therefore be used to explain the speckle, i.e., the variability between adjacent pairs of cells across the landscape.

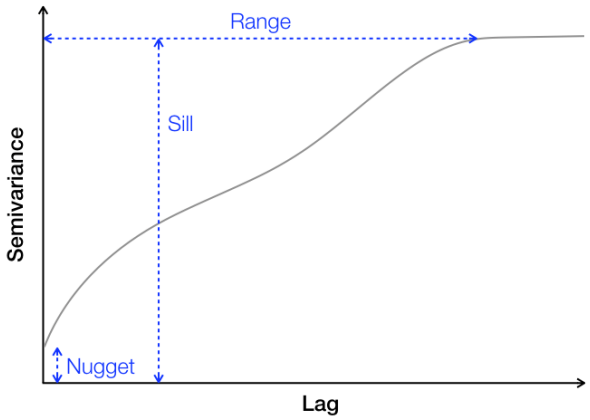

Figure 2. Semivariogram

In our case, the attributes of interest (Z) are external and internal temperatures. We would expect locations near each other to be (on average) fairly similar (i.e., correlated). We set the sampling interval distance of the semivariogram, i.e., the lag (h) to 10 km, a distance conveniently greater than that between adjacent grid locations. The resulting maps and semivariograms for T_{ex}^{mean} and $T_{in,s}^{mean}$ shown in Figure 3 are consistent with our assumptions. The ranges of the semivariogram for eastings for T_{ex}^{mean} and $T_{in,s}^{mean}$ are seen to be similar, at approximately 75 km. The nugget for northings and eastings are 0.26 (°C^2) and 0.18 (°C^2) for T_{ex}^{mean} respectively; and 0.19 (°C^2) and 0.13 (°C^2) for $T_{in,s}^{mean}$ respectively. These values are negligibly small, which reflects the observation that the differences of annual average temperatures between adjacent grids appears small in most regions and the images

in Figure 3 appear free of speckle, suggesting that in most cases 5 km would seem to be a sensible resolution for the production of weather files for the UK.

Returning to the temperature predictions, it is noticeable that the spatial variations in T_{ex}^{mean} shown in Figure 3 is similar to that found in the topographic variation presented in Figure 1 with an additional effect of latitude, as expected, suggesting that the spatial variability T_{ex}^{mean} is realistic. We can therefore conclude that pTRYs are suitable for assessing spatial variation in year-round average temperatures, building energy consumption, etc.

As previously discussed, much of the variability found in the temperature time series across the UK is due to altitude. Figure 4A shows the same data as Figure 3A, but after removing the altitude effect (by applying the same environmental lapse rate), the perturbation caused by the major cities is now even more evident. Figure 4B shows rise in $T_{ex}^{mean}$of pTRYs for the 2080s relative to the control period, i.e., 1970s. It is clear that the expected rise is not uniform. Figure 4C presents absolute differences between the T_{ex}^{mean} shown in Figure 3A and that shown in Figure 1D, i.e., the error in T_{ex}^{mean} of the adjusted CIBSE TRYs. Though there would be an offset in the overall errors due to warmer climate in the 2080s, it can be inferred from the spatial variability of the error that using the adjusted CIBSE TRYs would lead to unrealistic spatial variation in T_{ex}^{mean}. For instance, the errors for major cities are significantly larger as the UHI effect was not considered in the adjusted CIBSE TRYs. Hence, building simulation with the current CIBSE TRYs will lead to inaccuracies especially for urban areas.

Maps of gas use for heating (kWh·m^{-2} per year) for the 1970s and 2080s for the reference building are presented in Figure 5, which illustrate one possible use for such data. As presented in Figure 5B, the difference between the 1970s and 2080s is not uniform across the landscape. Compared to the 1970s, the heating energy in the 2080s was projected to be 23.5% lower on average (with a range from -14% to -39% across the landscape). The mean reduction of 23.5% is in line with estimations from previous studies [5, 57-59], however the wide range predicted once more points to the need to use high resolution weather files when setting local policy.

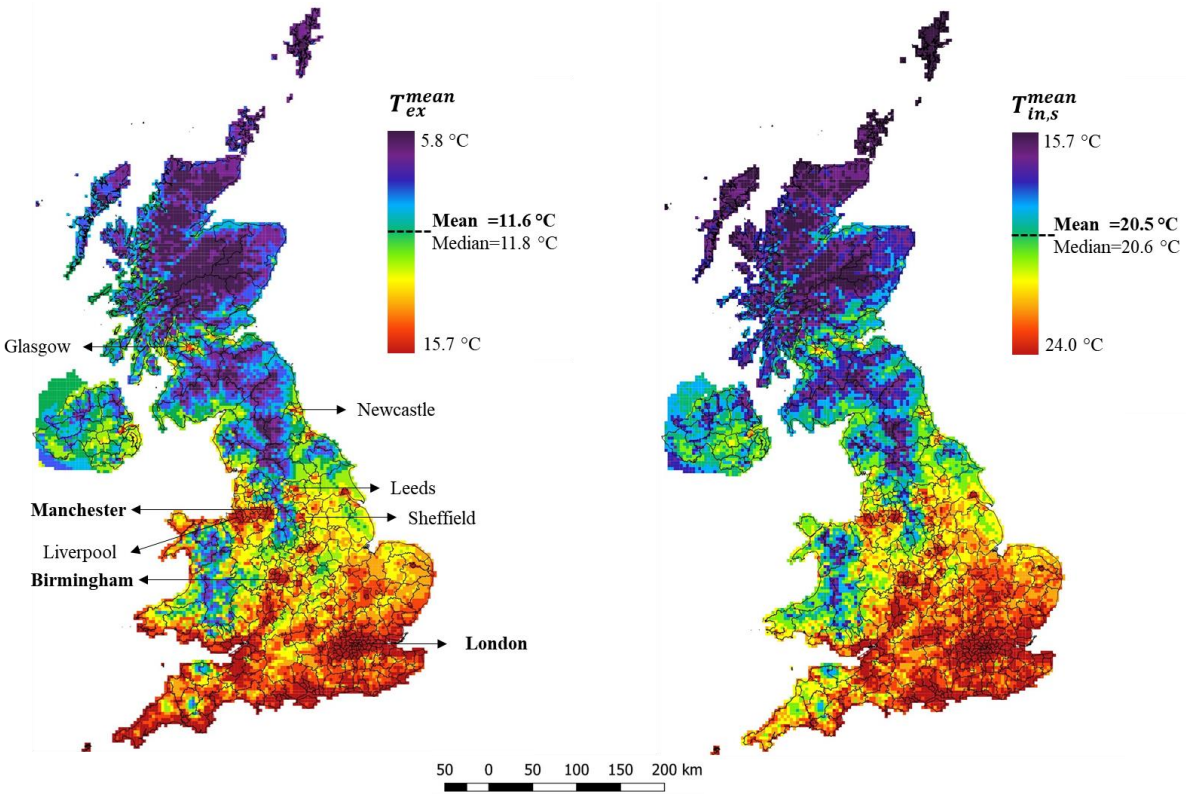

A) Whole-year **external** mean temperatures

B) Summertime **internal** mean temperatures of the reference house

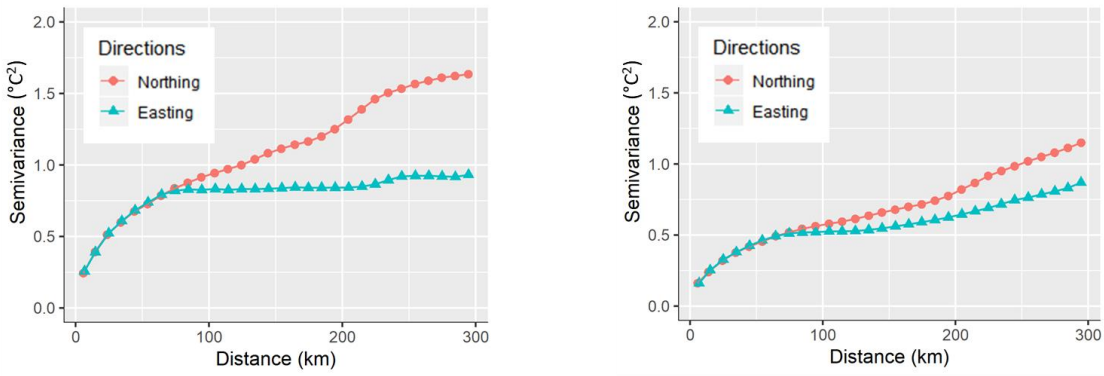

C) Semivariogram for T_{ex}^{mean}

D) Semivariogram for $T_{in,s}^{mean}$

Figure 3. A) shows the spatial variation in the whole-year external mean temperatures of pTRY (i.e., T_{ex}^{mean} of the 50th percentile TRYs for the 2080s); B) shows the resultant summertime internal mean temperatures ($T_{in,s}^{mean}$) found in the reference building; and C) and D) are their respective semivariograms. Quantile map classification was used so that each class contained approximately the same number of grids.

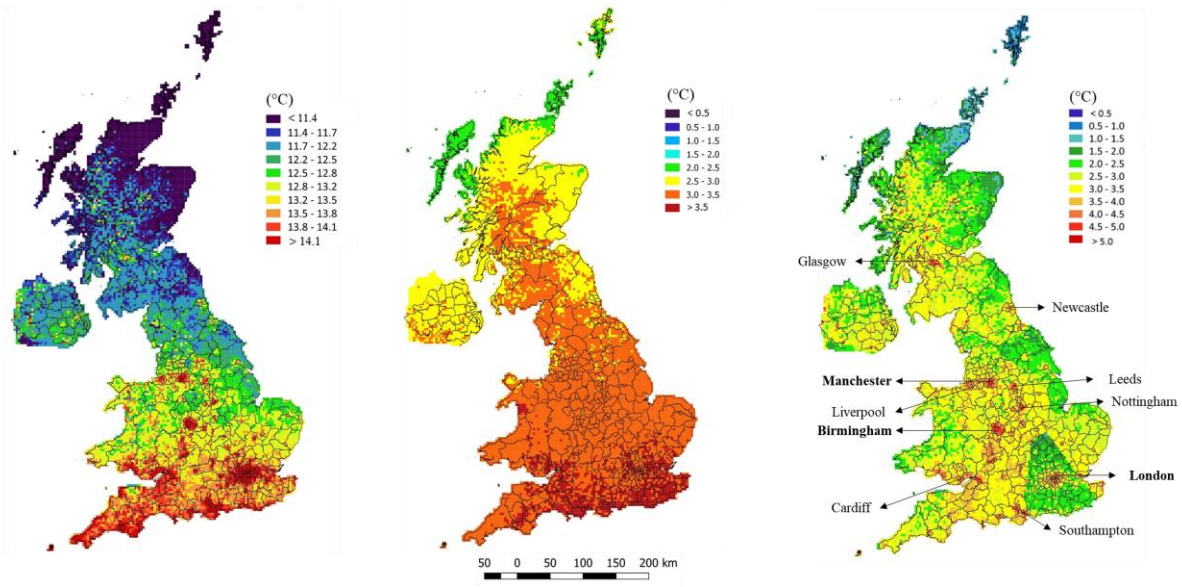

A) $T^{mean}_{50th\,TRY\_2080s}$ without altitude effect for the 2080s

B) Temperature rise (ΔT^{mean}) in the 2080s relative to the 1970s

C) Errors found in spatial variation in T^{mean}_{ex} for the adjusted CIBSE TRYs

Figure 4. A) shows the mean temperature of pTRY (i.e., the 50th percentile TRYs for the 2080s) after removing the effect of altitude; B) shows the rise in temperature in the 2080s relative to the 1970s under a medium emission scenario; C) shows the difference between the T^{mean}_{ex} shown in Figure 3A and in Figure 1D, i.e., the error caused by assuming only 14 locations, even if one adjusts for altitude.

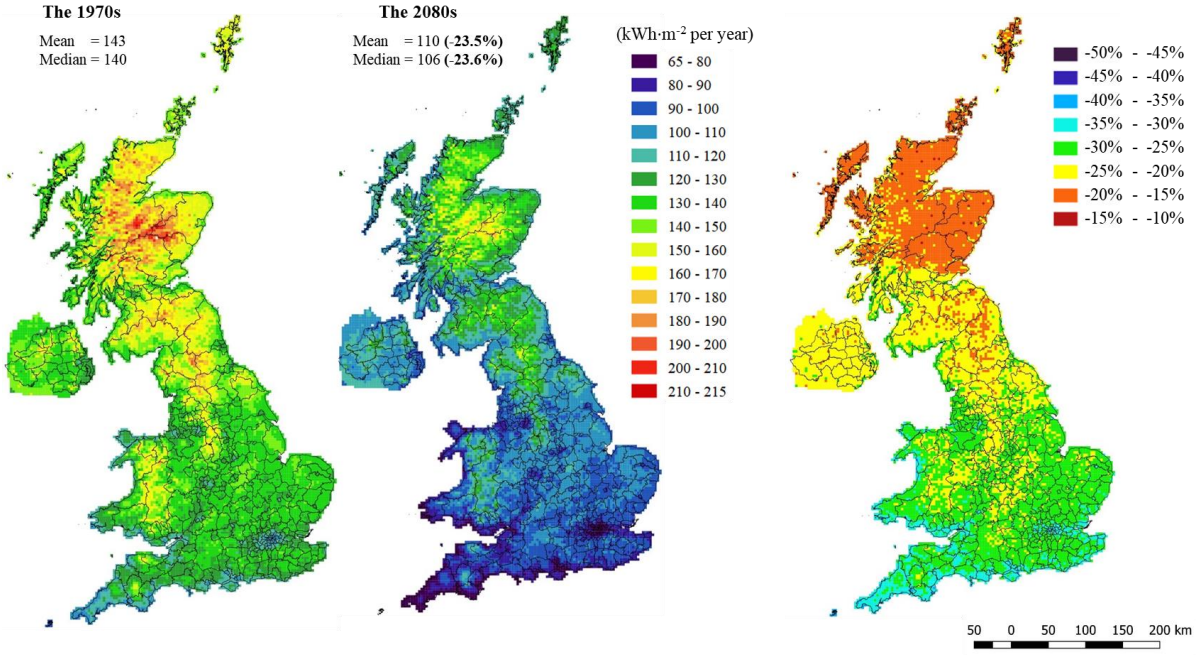

A) Gas use for heating (kWh·m^{-2} per year)

B) Reduction in gas use for heating (%)

Figure 5. A) shows gas use for heating (kWh·m^{-2} per year) in the reference building for the control year (i.e., the 1970s) and for the 2080s; B) shows the reduction (%) in gas use for heating in the 2080s relative to the 1970s.

4.3. Limitation of pTRY in representing spatial variability of external maximum and minimum temperatures

From the above, it would appear that the pTRYs based on the weather data generated from the SUWG reasonably reflect true spatial variability. This would indicate the potential to investigate how buildings might typically perform into the future, allowing the creation of highly localised policy that is both sensible and cost-effective.

The spatial distribution of the maximum hourly temperature (i.e.,$T_{ex}^{max} = \max(T_1, T_2, \dots T_{8760})$) and minimum hourly temperature (i.e.,$T_{ex}^{min} = \min(T_1, T_2, \dots T_{8760})$) of the pTRY (the 50th percentile TRY for the 2080s) are shown in Figure 6. It is clear that the distribution of temperatures is unrealistic, with a highly speckled appearance, in contrast with the common sense expectation that two adjacent places would have similar maximum and minimum temperatures. This is confirmed by the nuggets found in the semivariograms, which are almost 10 times those of Figure 3: 2.84 (°C^2) and 2.79 (°C^2) for T_{ex}^{max} for northings and eastings respectively, and 1.58 (°C^2) and 1.43 (°C^2) for T_{ex}^{min} respectively for northings and eastings. Thus, the pTRY is not suitable for use in mapping extremes. This is unsurprising as the method used to create a TRY is based on neither the maximum nor minimum one-hour temperature found in the time series.

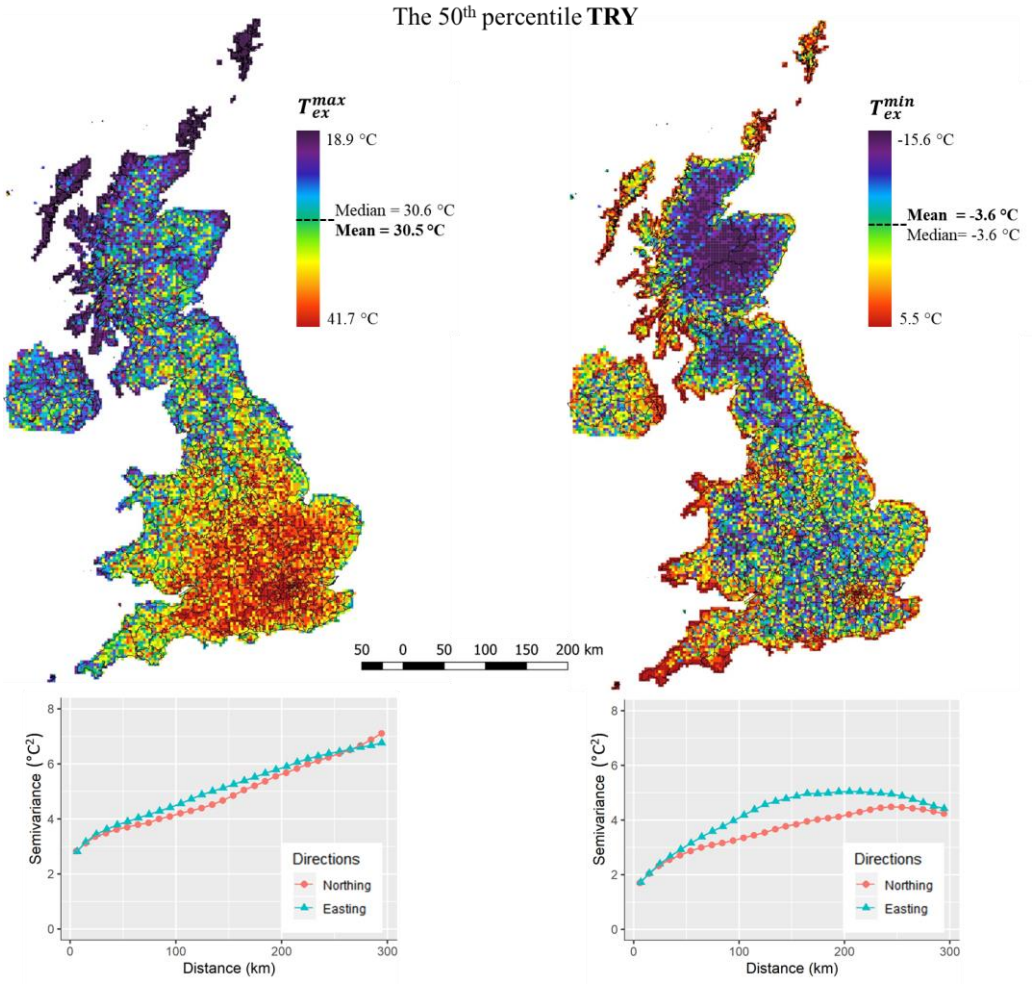

Figure 6. Spatial variation in the maximum and minimum temperatures (T_{ex}^{max} and T_{ex}^{min}) of pTRY (the 50th percentile TRY for the 2080s).

5. Creation of new pTRYs (pTRY-max and pTRY-min) at a 5 km by 5 km resolution

Current and future probabilistic TRYs (pTRY) consist of the most average months, as selected by the FS statistic [17, 19]. Hence the TRY method can ensure pTRYs are representative of the typical monthly situation. However, as shown above, there is no guarantee that any time series so generated will include a spatially consistent set of T_{ex}^{max} and T_{ex}^{min}. Therefore, these pTRYs are inappropriate in exploring the spatial variability of T_{ex}^{max} and T_{ex}^{min} across the landscape, or the impact of maximum or minimum temperatures on buildings or other systems. Hence we propose a new method for creating spatially consistent time series which contain realistic and typical maximum and minimum one-hour temperatures, and term these: pTRY-max and pTRY-min respectively. To be in line with the original TRY method, pTRY-max and pTRY-min are also composed of twelve months selected from potentially different sample years. Twelve months in the pTRY-max and pTRY-min were selected based on the maximum and minimum hourly temperatures respectively. For instance, the January which contained the typical maximum hourly temperature was selected from a set of 30 year-long climate data based on:

$$Diff(m,i) = abs\left| \; T_{m,i}^{max} - \overline{T_{m,N}^{max}} \; \right| \tag{2}$$

and

$$\overline{T_{m,N}^{max}} = \frac{\sum_{i=1}^{N} T_{m,i}^{max}}{N} \tag{3}$$

where, $T_{m,i}^{max}$ is the maximum hourly temperature of a month m in a sample year $i \in N$ (e.g., $T_{Jan,1}^{max} = \max(T_1, T_2, \ldots T_{31\times24})$) and N is the length of the period in years (in our case 30 years), $\overline{T_{m,N}^{max}}$ is the averaged maximum hourly temperature over all Januaries from a set of N year-long data, and $Diff(Jan,i)$ is the absolute difference between them. The January with the least $Diff(Jan,i)$ was selected from each set. So, 100 Januaries could be selected from 100 sets of 30 year-long data generated by the SUWG. Then, the 100 Januaries were ranked based on ascending order of T_{ex}^{max}. Finally, the January, February and so on with the same percentile rank were concatenated to form a probabilistic TRY-max. That is, each calendar month of the pTRY-max contains a typical T_{ex}^{max} for that month. Likewise, the probabilistic TRY-min has been created based on T_{ex}^{min}.

Figure 7 presents the spatial variation in T_{ex}^{max} for pTRY-max and the spatial variation in T_{ex}^{min} for pTRY-min. From the map of T_{ex}^{min} (on the right) it is clear that the coastline is warmer than inland; furthermore, as expected the UHI effect is much stronger compared to ones shown over the map of T_{ex}^{max} (on the left), and the map of T_{ex}^{mean} shown in Figure 6. Semivariances shown in Figure 7 are smaller than the ones shown in Figure 6 for the same lags. For instance, the semivariance for a distance of 100 km shown in Figure 7 is less than 2 (°C^2) which is half of the semivariance shown in Figure 6. In addition, the nuggets of the semivariograms for easting are 0.28 (°C^2) and 0.12 (°C^2) for T_{ex}^{max} and T_{ex}^{min} respectively, close to those given in Figure 3. That is, the spatial continuity for both T_{ex}^{max} of pTRY-max and T_{ex}^{min} of pTRY-min are dramatically improved compared to Figure 6, with adjacent cells having similar values. Maps and semivariograms for other weather variables can be found in Append.

It should be noted that the purpose of pTRY-max and pTRY-min is not to allow the study of rare extreme conditions, e.g., heat waves and cold snaps, but to provide spatially consistent *typical* maximum and minimum conditions in line with the TRY philosophy, thereby allowing external and internal conditions at the typically coldest or hottest temperature to be studied.

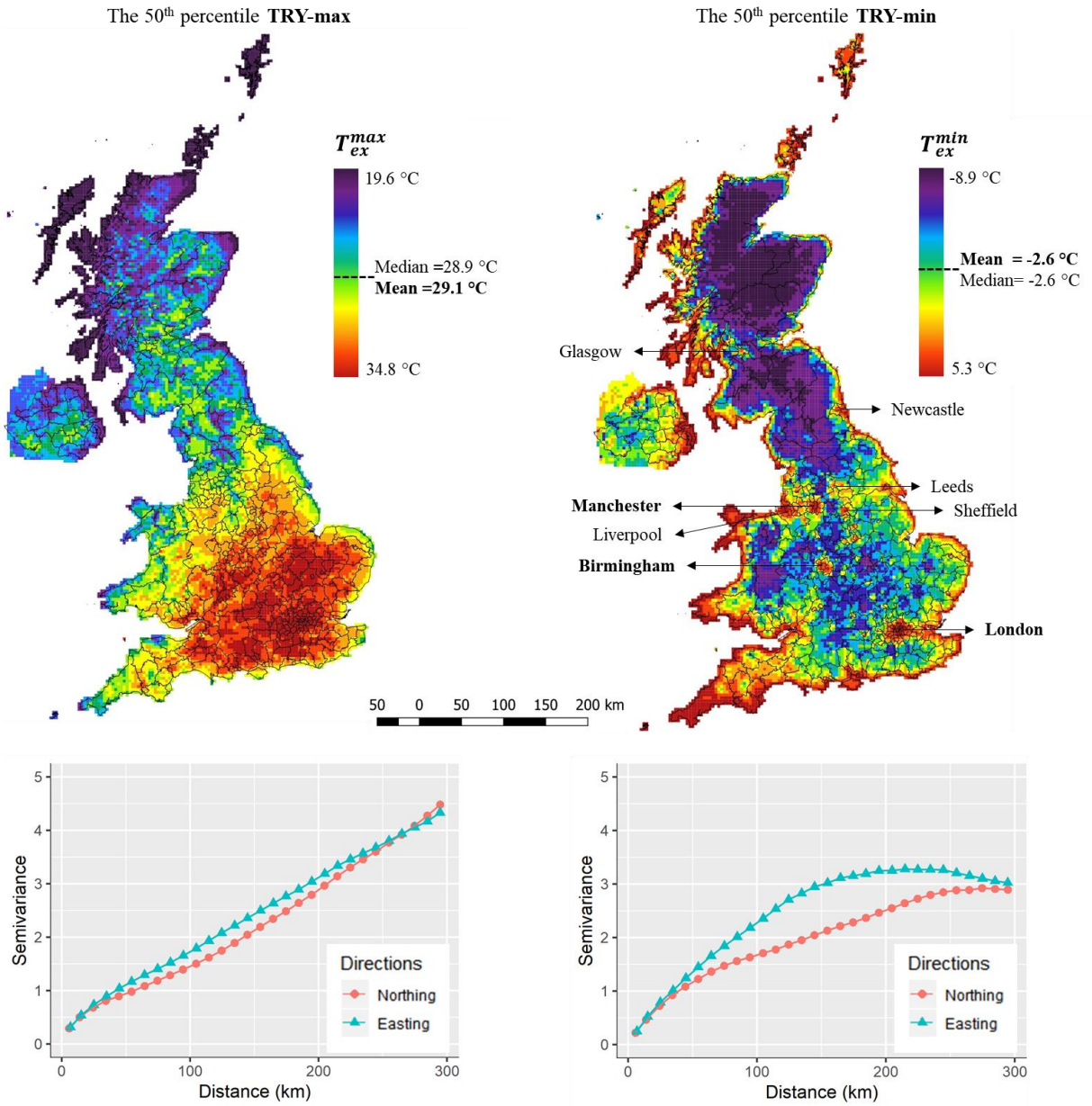

Figure 7. Spatial variation in the maximum hourly temperatures of pTRY-max (on the left) and the minimum temperatures of pTRY-min (on the right) for the 2080s.

An important question, however, is that whether the T_{ex}^{mean} and $T_{in,s}^{mean}$ of the pTRY-max and pTRY-min are similar to that of pTRY. Figure 8 shows that the spatial variation in T_{ex}^{mean} of pTRY-max and pTRY-min are extremely similar to that of pTRY across the UK. It is encouraging that the spatial continuity, i.e., the nuggets and ranges of the semivariograms are almost identical. Figure 9 presents the spatial variation in $T_{in,s}^{mean}$ for the reference building during the summer. Again, the spatial variation in $T_{in,s}^{mean}$ for pTRY, pTRY-max and pTRY-min are similar across the landscape. Moreover, the differences of median T_{ex}^{mean} between them are less than 0.3°C as can be seen in Figure 10. Dynamic thermal simulations with pTRY, pTRY-max and pTRY-min have been carried out for all of the 11,326 grid locations, and differences of median $T_{in,s}^{mean}$ between them are negligible as can be seen from the data in Figure 10. Thus, it would appear that pTRY-max and pTRY-min well represent the year round average temperature, as well as the maximum and minimum temperatures (respectively).

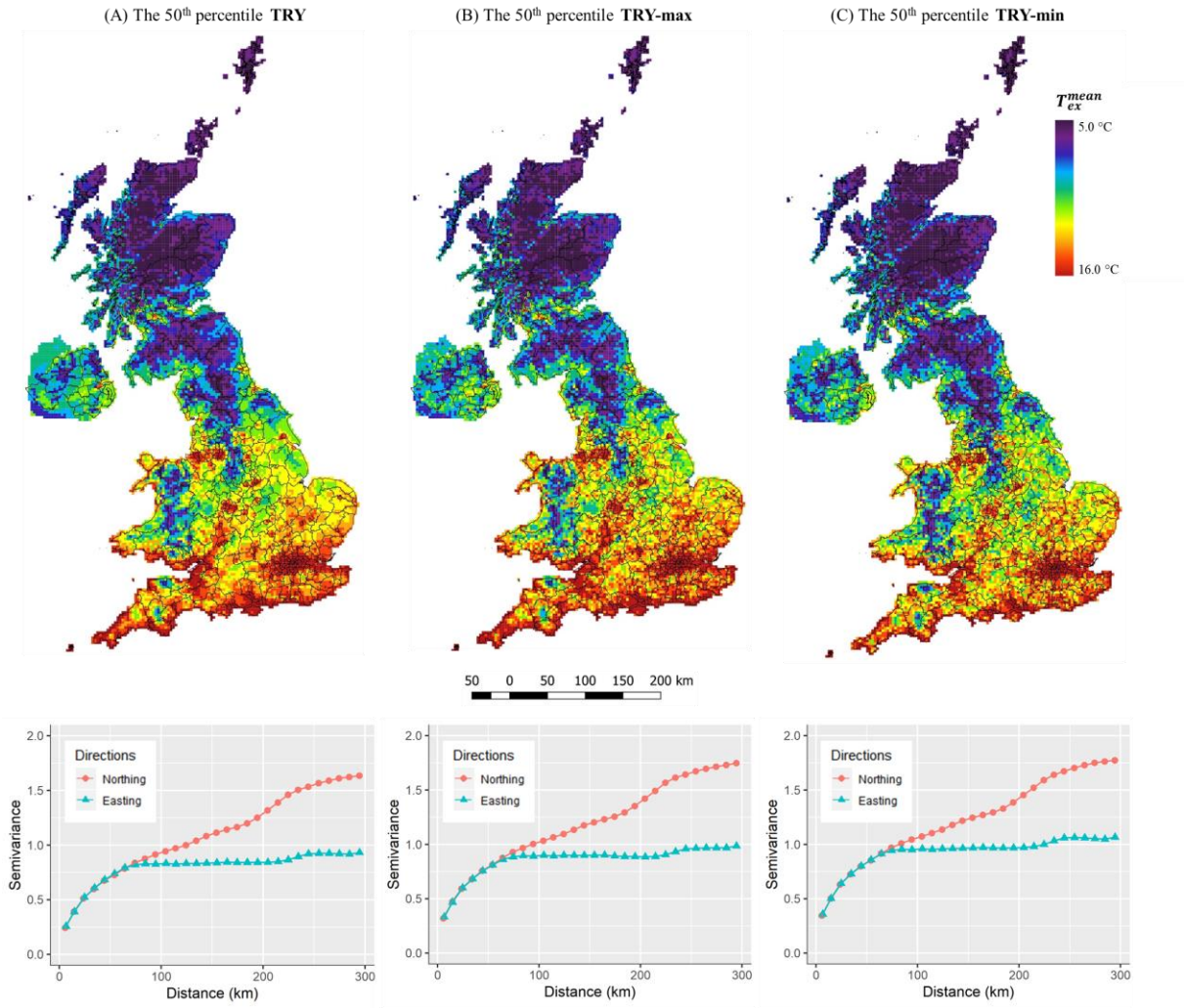

Figure 8. Spatial variation in the mean temperature (T_{ex}^{mean}) of pTRY, pTRY-max and pTRY-min for the 2080s.

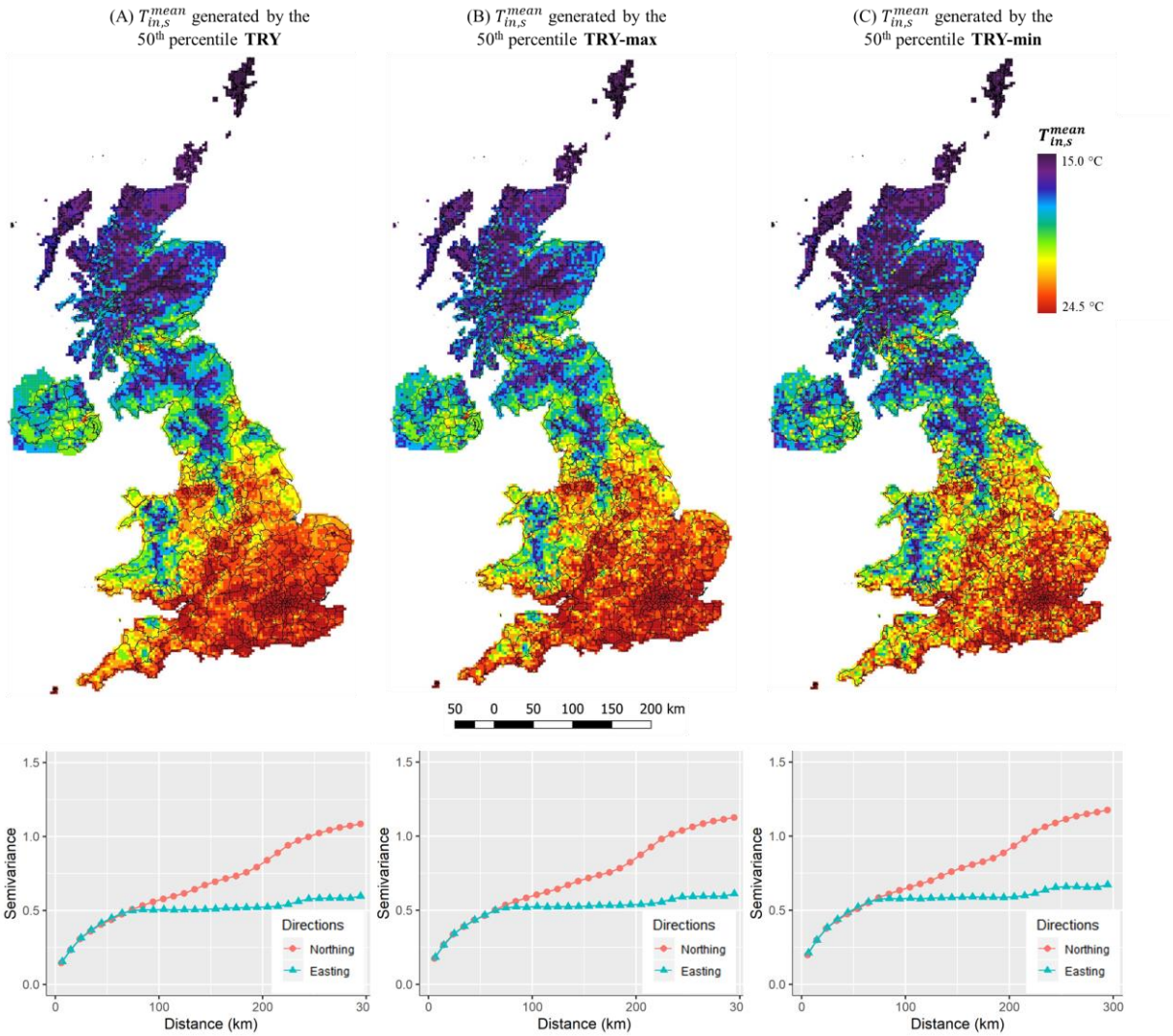

Figure 9. Maps of summertime internal mean temperature ($T_{in,s}^{mean}$) of the reference building generated by pTRY, pTRY-max and pTRY-min for the 2080s.

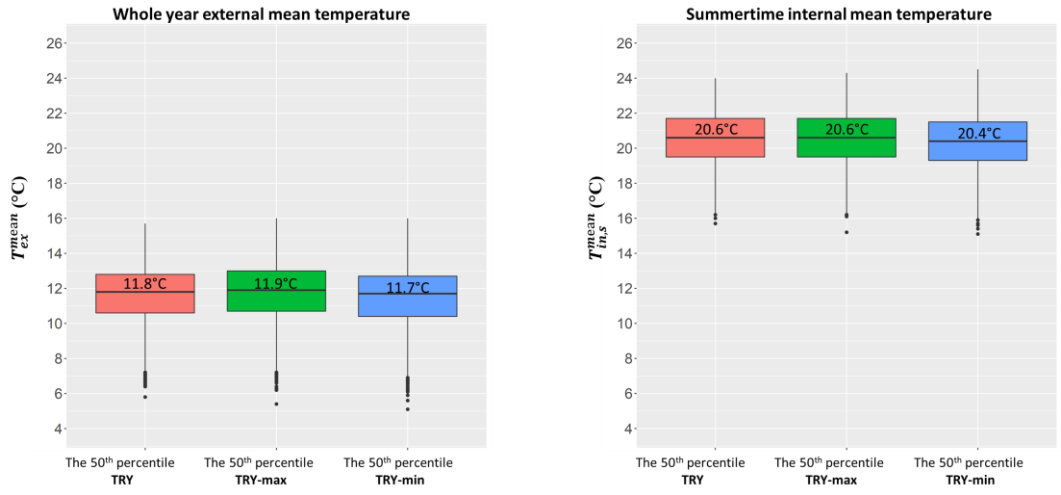

Figure 10. Comparison between pTRY, pTRY-max and pTRY-min. Boxplots constructed using temperatures of the 50th percentile TRY, TRY-max and TRY-min (on the left) and summertime internal temperatures generated by them (on the right) for all 11,326 grid locations.

6. Use of the files

By providing pTRYs at 11,326 locations energy modellers and those looking at the performance of buildings can proceed for the first time knowing that they are using weather representative of the local situation. Others will be interested in how energy use in buildings or internal temperatures in free running buildings changes across the landscape. The pTRY can be used for assessing year-round energy performance of buildings under average conditions, while pTRY-max and pTRY-min might be used for looking at typical maximal and minimal conditions, for instance, in looking at how peak heating and cooling load changes across the landscape. One impressive aspect of these new files is the clear identification of an UHI. The weather files can be downloaded from a website (https://colbe.bath.ac.uk/) by providing a postcode or latitude and longitude of the location of interest. The following files can be downloaded: 1) typical years such as pTRY, pTRY-max, pTRY-min for the 1970s, 2020s and 2080s, and 2) warmer than typical years represented by probabilistic Design Summer Years (pDSY) [19] and probabilistic Hot Summer Years (pHSY) [24] for the 1970s, 2020s and 2080s.

7. Conclusion

The aim of this work was to produce localised test reference years for building simulations across the whole of the UK and examine spatial variability and to discover if 5 km was a sensible resolution. For the first time, pTRYs were created for 11,326 grid locations based on approximately 30 TB of synthetic weather data generated by the updated SUWG which takes topographic effects into account. The SUWG has incorporated the urban anthropogenic component so that the synthetic weather data from the SUWG could be used to explore the UHI effect. Indicative dynamic thermal simulations for 11,326 locations have also been carried out. The pTRYs show a realistic spatial distribution, as measured by their semivariograms. The UHI effect is clearly evident and the realistic spatial variation also makes sensible predictions in the spatial variation in the thermal performance of a reference building. Hence, we believe the pTRYs can be used to examine the spatial variability of conditions within buildings at an unprecedented resolution. The *nuggets* for northings and eastings are negligibly small, which reflects the reality that the differences of annual average temperatures between adjacent grids appear small in most regions, suggesting that 5 km is a sensible resolution for the production of weather files for the UK.

One unanticipated finding was that pTRY showed limitations in mapping *maximum* and *minimum* hourly temperatures with poor spatial continuity and unrealistic differences between adjacent grids. Hence a new method was proposed to create new pTRY (i.e. pTRY-max and pTRY-min) for the study of peak heating and cooling loads and other situations requiring a one-hour metric.

Although these files were produced for building thermal modelling, and to support national built environment policy, they are likely to be of interest to other disciplines including studies of renewable energy generation, crop yields and climate resilience.

Acknowledgements and data access

This research was carried out as part of the EPSRC funded project COLBE (The Creation of Localised and Future Weather for the Build Environment, EP/M021890/1). We are grateful to Professor Chris Kilsby and Dr Vassilis Glenis at Newcastle University for providing the updated Spatial Urban Weather Generator. The data displayed in the maps can be found at https://doi.org/10.15125/BATH-00666 [60].

Appendix

Notation

IPCC	Intergovernmental Panel on Climate Change
SRES	Special Report on Emissions Scenarios [61]
CIBSE	The Chartered Institution of Building Services Engineers
CIBSE TRY	CIBSE Test Reference Year
UKCP09	The UK Climate Projections 2009
SUWG	The Spatial Urban Weather Generator, an updated version of the UKCP09 Weather Generator
pTRY	Probabilistic Test Reference Year
pTRY-max	New probabilistic Test Reference Year containing a typical hourly maximum temperature
pTRY-min	New probabilistic Test Reference Year containing a typical hourly minimum temperature

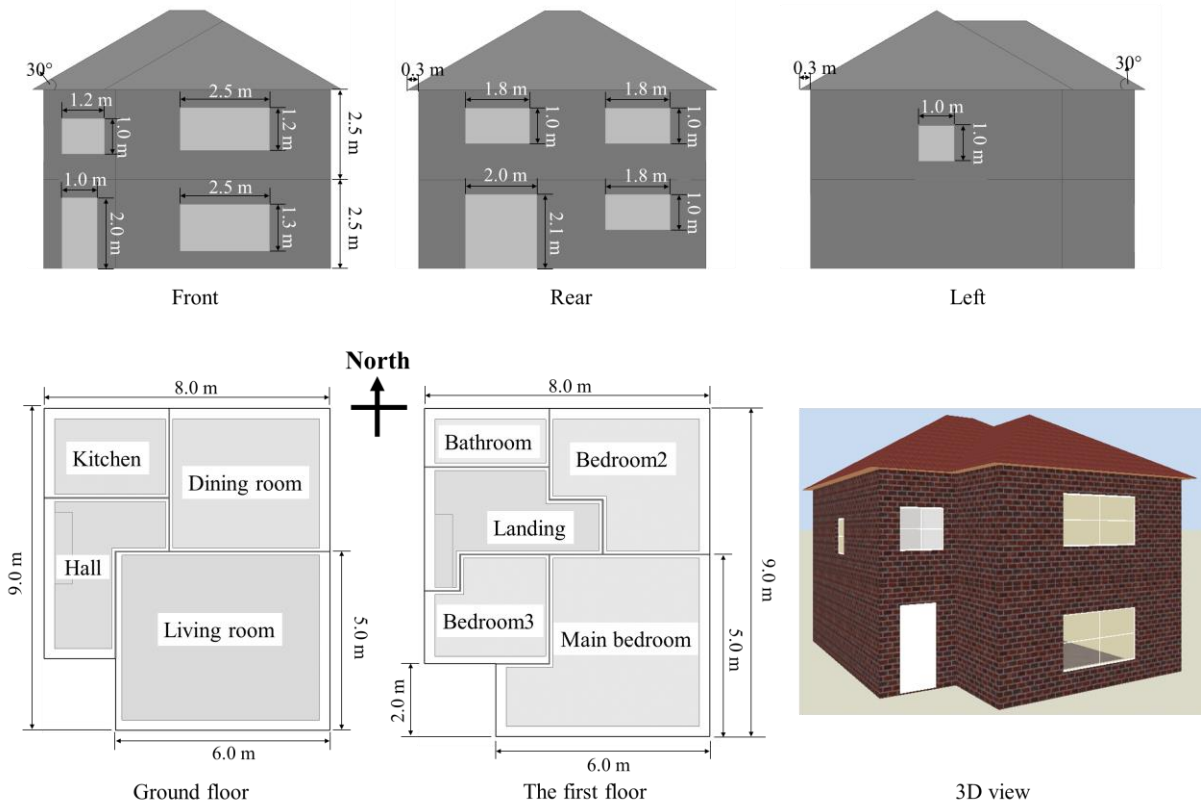

Figure A-1. Geometry, floor plan and glazing dimensions of the detached house

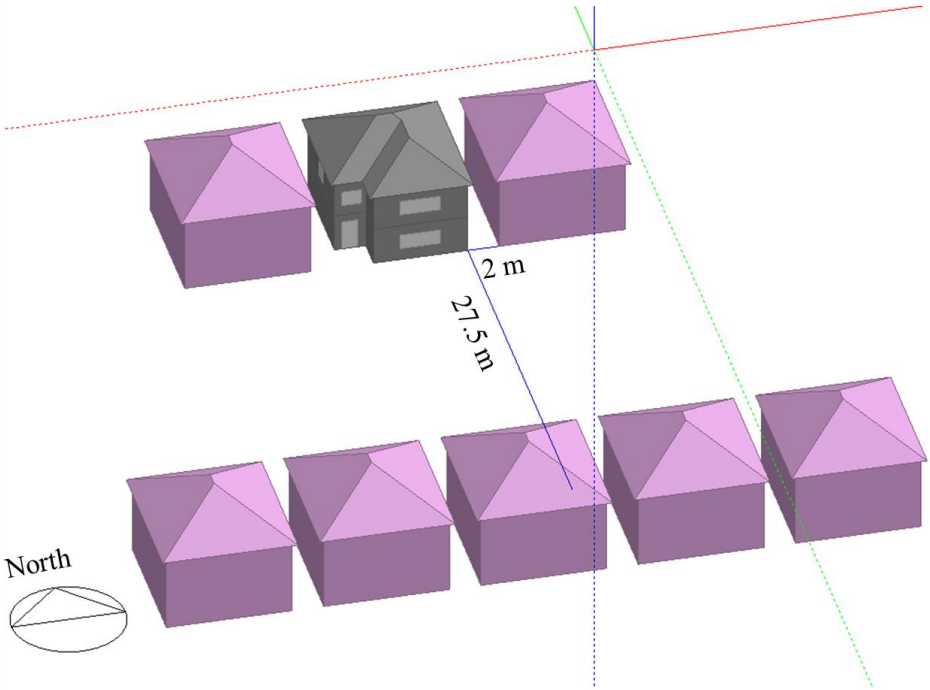

Figure A-2. Illustration of surrounding buildings. The distance between adjacent houses and the privacy distance between facing houses are in accordance with Residential Design Guide [38].

Table A-1. Construction details

			Construction	U-value (W·m²K)
External wall	105	mm	brickwork outer leaf	1.5
	100	mm	cavity ventilated	
	105	mm	brick, inner leaf	
	13	mm	plaster	
Internal partition	13	mm	lightweight plaster	1.1
	100	mm	lightweight concrete	
	13	mm	lightweight plaster	
Internal floor	12.5	mm	plasterboard (ceiling)	1.6
	50	mm	air layer	
	65	mm	cast concrete	
	25	mm	wood block	
Ground floor	500	mm	clay underfloor	1.1
	150	mm	concrete roof/floor slab	
	50	mm	flooring screed	
Pitched roof	10	mm	concrete roof tiles	2.0
	-	-	roof space	
	12.5	mm	plasterboard (ceiling)	

Note: thermal conductivity, density and specific heat capacity of building materials can be found in CIBSE Guide A [62].

Table A-2. Window and door characteristics

			Construction	U-value (W·m²K)
Single glazing	6	mm	generic clear glass	4.8 (SHGC=0.85)
Wooden frame	20	mm	wood	3.6
Door	35	mm	painted oak	2.8

Table A-3. Effective air change rate (ach) for each zone

Zones		Cross ventilation	Night-time ventilation	The maximum air change rate (ach)
Ground floor	Living (30 m²) Dining (18 m²) Kitchen (8.75 m²) Hall (11.25 m²)	Possible	Only possible during occupied hours for security issue	4
First floor	Main bedroom (25.5 m²) Bedroom 2 (15.75 m²) Bedroom 3 (9.5 m²) Bathroom (5.6 m²)	Internal doors are closed when occupied	Possible	2.5

Table A-4. Occupancy and equipment profiles

Zones	Number of occupants	Metabolic rate (W/person) & Occupied hours		Equipment (W) & Schedule		Lighting schedule (15 W·m^2)	Hot water schedule (80 W)
Living	2	108 (seated)	17:00-22:00	160 (TV)	17:00-18:00 19:00-22:00	17:00-22:00	-
Dining	0	-	-	60 (Fridge)	00:00-24:00	08:00-09:00	-
Kitchen	0	-	-	160 1600 (cooker)	07:00-08:00 18:00-1900	07:00-08:00 18:00-21:00	00:00-24:00
Hall	0	-		-	-	07:00-08:00 18:00-21:00	-
Main bedroom	2	72 (sleeping)	22:00-07:00	-	-	-	-
Bedroom 2	1	55	21:00-07:00	100 (PC)	-	-	-
Bedroom 3	1	55	21:00-07:00	-	-	-	-
Bathroom	0	-	-	20	07:00-08:00 20:00-2100	07:00-08:00 20:00-2100	00:00-24:00

Note: the equipment and lighting schedules were modified from BEPAC Technical Note 90/2 [36] to be in line with the latest survey on energy use in English homes [51]; the main bedroom was for a couple (i.e. adults) while bedroom 2 and 3 were for children.

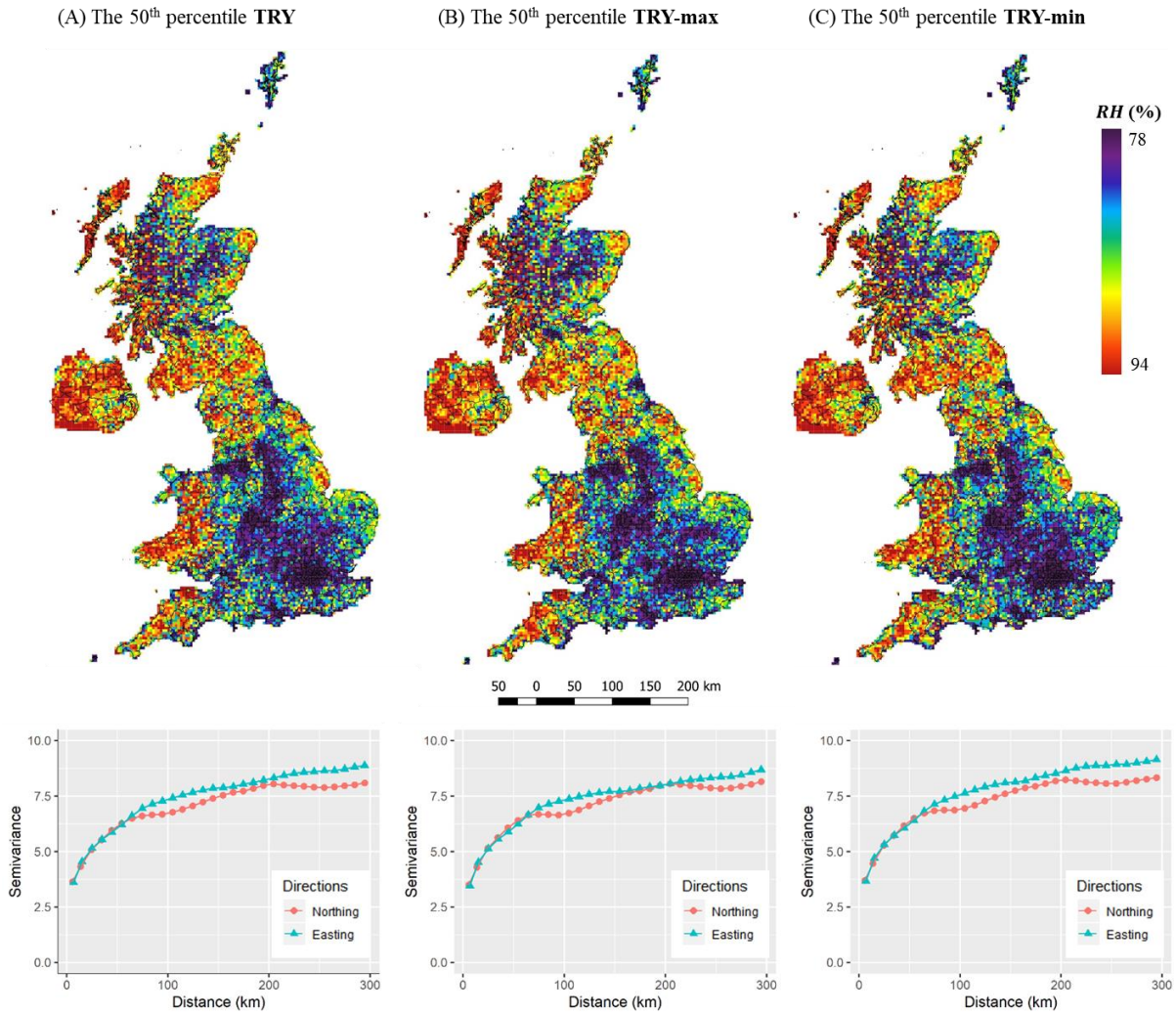

Figure A-3. Spatial variation in the external mean relative humidity (RH) of pTRY, pTRY-max and pTRY-min for the 2080s.

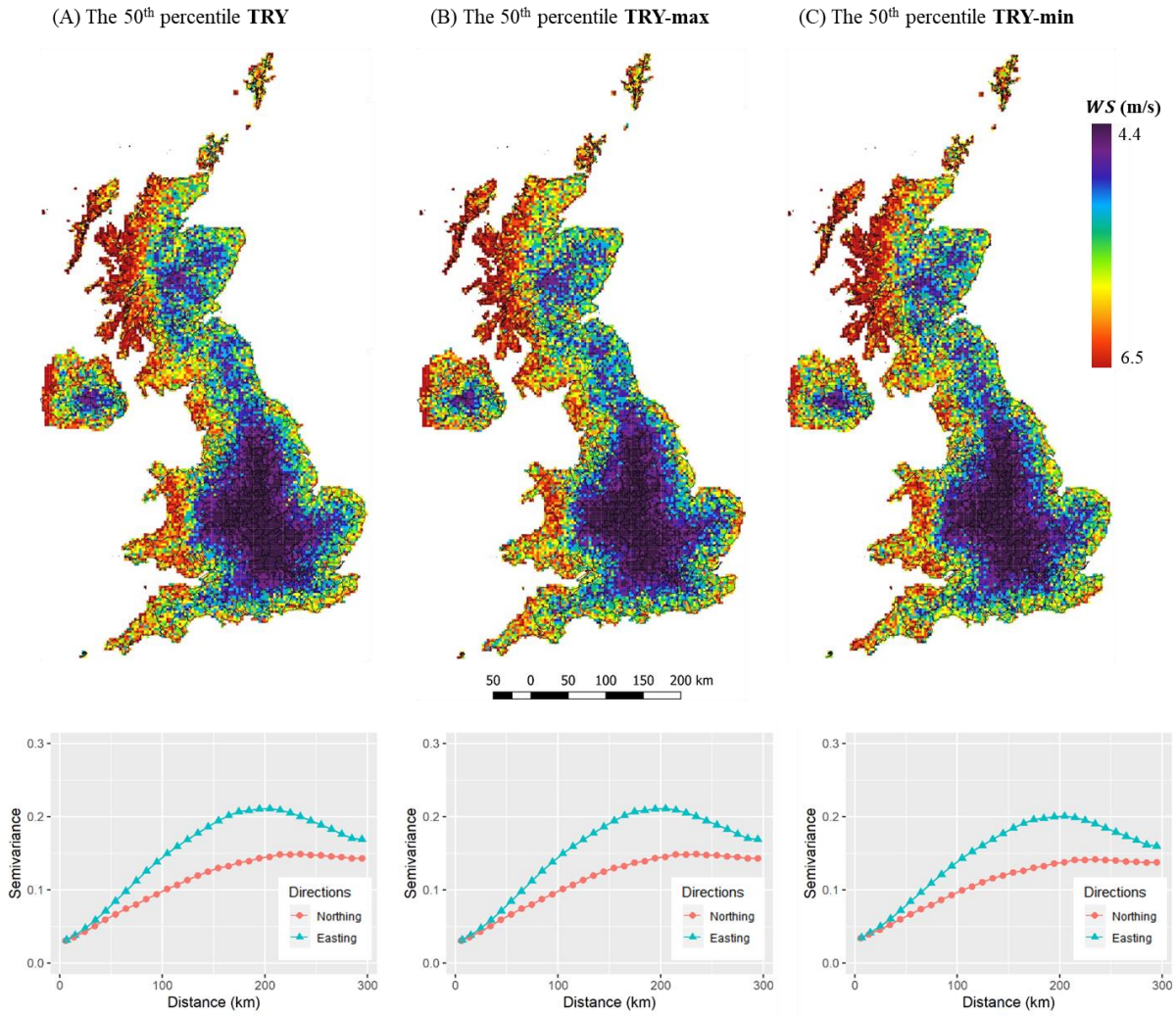

Figure A-4. Spatial variation in the mean wind speed (WS) of pTRY, pTRY-max and pTRY-min for the 2080s.

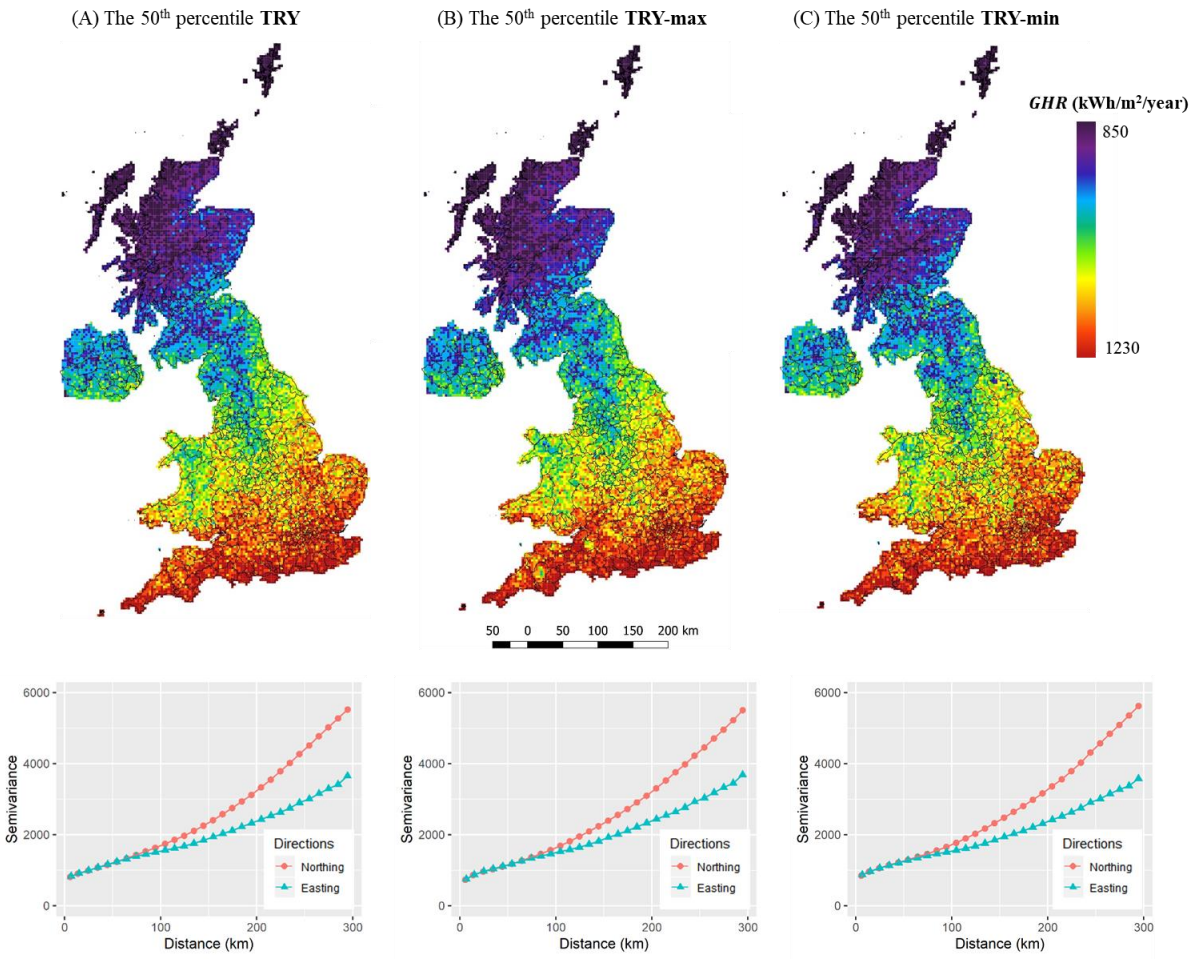

Figure A-5. Spatial variation in the whole-year global horizontal irradiation (GHR) of pTRY, pTRY-max and pTRY-min for the 2080s.

References

1. Liu C, Kershaw T, Fosas D, et al. High resolution mapping of overheating and mortality risk. *Building and Environment* 2017; 122: 1-14. DOI: https://doi.org/10.1016/j.buildenv.2017.05.028.
2. Taylor J, Davies M, Mavrogianni A, et al. The relative importance of input weather data for indoor overheating risk assessment in dwellings. *Building and Environment* 2014; 76: 81-91. DOI: http://doi.org/10.1016/j.buildenv.2014.03.010.
3. Taylor J, Wilkinson P, Picetti R, et al. Comparison of built environment adaptations to heat exposure and mortality during hot weather, West Midlands region, UK. *Environment International* 2018; 111: 287-294. DOI: https://doi.org/10.1016/j.envint.2017.11.005.
4. Du H, Underwood C and Edge J. Generating test reference years from the UKCP09 projections and their application in building energy simulations. *Building Services Engineering Research and Technology* 2011; 33: 387-406. DOI: http://doi.org/10.1177/0143624411418132.
5. Eames M, Kershaw T and Coley D. The appropriate spatial resolution of future weather files for building simulation. *Journal of Building Performance Simulation* 2012; 5: 347-358. DOI: https://doi.org/10.1080/19401493.2011.608133.
6. Gupta R and Gregg M. Using UK climate change projections to adapt existing English homes for a warming climate. *Building and Environment* 2012; 55: 20-42. DOI: http://doi.org/10.1016/j.buildenv.2012.01.014.
7. Jenkins K, Hall J, Glenis V, et al. Probabilistic spatial risk assessment of heat impacts and adaptations for London. *Climatic Change* 2014; 124: 105-117. journal article. DOI: http://doi.org/10.1007/s10584-014-1105-4.
8. Holmes MJ and Hacker JN. Climate change, thermal comfort and energy: Meeting the design challenges of the 21st century. *Energy and Buildings* 2007; 39: 802-814. DOI: https://doi.org/10.1016/j.enbuild.2007.02.009.
9. Kershaw T, Eames M and Coley D. Assessing the risk of climate change for buildings: A comparison between multi-year and probabilistic reference year simulations. *Building and Environment* 2011; 46: 1303-1308. DOI: http://doi.org/10.1016/j.buildenv.2010.12.018.
10. Lomas KJ and Ji Y. Resilience of naturally ventilated buildings to climate change: Advanced natural ventilation and hospital wards. *Energy and Buildings* 2009; 41: 629-653. DOI: https://doi.org/10.1016/j.enbuild.2009.01.001.
11. Mavrogianni A, Wilkinson P, Davies M, et al. Building characteristics as determinants of propensity to high indoor summer temperatures in London dwellings. *Building and Environment* 2012; 55: 117-130. DOI: http://doi.org/10.1016/j.buildenv.2011.12.003.
12. McLeod RS, Hopfe CJ and Kwan A. An investigation into future performance and overheating risks in Passivhaus dwellings. *Building and Environment* 2013; 70: 189-209. DOI: http://doi.org/10.1016/j.buildenv.2013.08.024.
13. Jenkins DP, Patidar S, Banfill PFG, et al. Probabilistic climate projections with dynamic building simulation: Predicting overheating in dwellings. *Energy and Buildings* 2011; 43: 1723-1731. DOI: http://doi.org/10.1016/j.enbuild.2011.03.016.
14. Patidar S, Jenkins DP, Gibson GJ, et al. Statistical techniques to emulate dynamic building simulations for overheating analyses in future probabilistic climates. *Journal of Building Performance Simulation* 2011; 4: 271-284. DOI: http://doi.org/10.1080/19401493.2010.531144.
15. Patidar S, Jenkins DP, Gibson GJ, et al. Analysis of probabilistic climate projections: heat wave, overheating and adaptation. *Journal of Building Performance Simulation* 2013; 6: 65-77. DOI: http://doi.org/10.1080/19401493.2012.684447.
16. Pyrgou A, Castaldo VL, Pisello AL, et al. Differentiating responses of weather files and local climate change to explain variations in building thermal-energy performance simulations. *Solar Energy* 2017; 153: 224-237. DOI: https://doi.org/10.1016/j.solener.2017.05.040.
17. Levermore GJ and Parkinson JB. Analyses and algorithms for new Test Reference Years and Design Summer Years for the UK. *Building Service Engineering Research and Technology* 2006; 27: 311-325. DOI: http://doi.org/10.1177/0143624406071037.

18. Eames M, Ramallo-Gonzalez A and Wood M. An update of the UK's test reference year: The implications of a revised climate on building design. *Building Services Engineering Research and Technology* 2015. DOI: http://doi.org/10.1177/0143624415605626.
19. Eames M, Kershaw T and Coley D. On the creation of future probabilistic design weather years from UKCP09. *Building Services Engineering Research and Technology* 2011; 32: 127-142. DOI: http://doi.org/10.1177/0143624410379934.
20. Jones PD, Kilsby CG, Harpham C, et al. *UK Climate Projections science report: Projections of future daily climate for the UK from the Weather Generator*. 2010. University of Newcastle, UK: University of Newcastle, UK.
21. Kilsby CG, Jones PD, Burton A, et al. A daily weather generator for use in climate change studies. *Environmental Modelling & Software* 2007; 22: 1705-1719. DOI: http://doi.org/10.1016/j.envsoft.2007.02.005.
22. Li Z-L, Tang B-H, Wu H, et al. Satellite-derived land surface temperature: Current status and perspectives. *Remote Sensing of Environment* 2013; 131: 14-37. DOI: http://doi.org/10.1016/j.rse.2012.12.008.
23. Mylona A. The use of UKCP09 to produce weather files for building simulation. *Building Services Engineering Research and Technology* 2012; 33: 51-62. DOI: http://doi.org/10.1177/0143624411428951.
24. Liu C, Kershaw T, Eames ME, et al. Future probabilistic hot summer years for overheating risk assessments. *Building and Environment* 2016; 105: 56-68. DOI: http://doi.org/10.1016/j.buildenv.2016.05.028.
25. Smith ST and Hanby V. Methodologies for the generation of design summer years for building energy simulation using UKCP09 probabilistic climate projections. *Building Services Engineering Research and Technology* 2012; 33: 9-17. DOI: http://doi.org/10.1177/0143624411429183.
26. Watkins R, Levermore G and Parkinson J. The design reference year - a new approach to testing a building in more extreme weather using UKCP09 projections. *Building Services Engineering Research and Technology* 2012; 34: 165-176. DOI: http://doi.org/10.1177/0143624411431170.
27. Watkins R, Levermore G and Parkinson J. Constructing a future weather file for use in building simulation using UKCP09 projections. *Building Services Engineering Research and Technology* 2011; 32: 293-299. DOI: http://doi.org/10.1177/0143624410396661.
28. Cowpertwait PSP, O'Connell PE, Metcalfe AV, et al. Stochastic point process modelling of rainfall. II. Regionalisation and disaggregation. *Journal of Hydrology* 1996; 175: 47-65. DOI: https://doi.org/10.1016/S0022-1694(96)80005-9.
29. Kilsby C, Jones P, Harpham C, et al. Spatial Urban Weather Generator for Future Climates. https://www.arcc-network.org.uk/wp-content/pdfs/ARCADIA-Spatial-urban-WG.pdf (2011, accessed 25 June 2018).
30. McCarthy MP, Harpham C, Goodess CM, et al. Simulating climate change in UK cities using a regional climate model, HadRM3. *International Journal of Climatology* 2012; 32: 1875-1888. DOI: http://doi.org/10.1002/joc.2402.
31. Allen R, Pereira L, Raes D, et al. Guidelines for computing crop water requirements-FAO Irrigation and drainage paper 56; FAO-Food and Agriculture Organization of the United Nations, Rome (http://www.fao.org/docrep). ARPAV (2000), La caratterizzazione climatica della Regione Veneto, Quaderni per. *Geophysics* 1998; 156: 178.
32. Eames M, Kershaw T and Coley D. On the creation of future probabilistic design weather years from UKCP09. *Building Services Engineering Research and Technology* 2010; 32: 127-142. DOI: 10.1177/0143624410379934.
33. Eames M, Kershaw TJ and Coley D. A comparison of future weather created from morphed observed weather and created by a weather generator. *Building and Environment* 2012; 56: 252-264. DOI: http://doi.org/10.1016/j.buildenv.2012.03.006.

34. Jentsch MF. *Viability of naturally ventilated buildings in the UK under predicted future summer climates*. University of Southampton, 2009.
35. DesignBuilder. https://designbuilder.co.uk/ (accessed 12 March 2019).
36. Allen E and Pinney A. *Standard dwellings for modelling: details of dimensions, construction and occupancy schedules (BEPAC Technical Note 90/2)*. Building Environmental Performance Analysis Club, Building Research Establishment, Watford, UK, 1990.
37. DCLG. *English Housing Survey Headline Report 2017-18*. 2019. Ministry of Housing, Communities and Local Government, London, UK.
38. Watford Borough Council. Residential Design Guide. Watford, UK2016.
39. BRE. Reduced data SAP for existing dwellings (RdSAP 2012 version 9.93). Watford, UK: Building Research Establishment, 2017.
40. US DOE. EnergyPlus (version 8.8.0), https://energyplus.net/ (accessed 12 March 2019).
41. Stephen R. *Airtightness in UK dwellings*. BRE Watford, 2000.
42. Johnston D, Wingfield J, Miles-Shenton D, et al. Airtightness of UK dwellings: some recent measurements. In: *RICS Foundation Construction and Building Research Conference; Ellis, R, Bell, M, Eds* 2004, p.13.
43. BRECSU. Good Practice Guide 224: Improving airtightness in existing homes. Building Research Energy Conservation Support Unit, BRE, Watford, UK1997.
44. BRE. The Government's Standard Assessment Procedure for Energy Rating of Dwellings (SAP 2012 version 9.92). Watford, UK: Building Research Establishment (BRE), 2014.
45. *CIBSE TM36 (2005) - Climate change and the indoor environment: impacts and adaptation*. The Chartered Institution of Building Services Engineers.
46. CIBSE. *CIBSE TM36, Climate change and the indoor environment: impacts and adaptation.(Pricipal authors: J.N. Hacker, M.J. Holmes, S.B. Belcher, G.D. Davies)*. 2005. The Chartered Institution of Building Services Engineers, London, UK.
47. Demanuele C, Mavrogianni A, Davies M, et al. Using localised weather files to assess overheating in naturally ventilated offices within London's urban heat island. *Building Services Engineering Research and Technology* 2012; 33: 351-369. DOI: http://doi.org/10.1177/0143624411416064.
48. Porritt SM, Cropper PC, Shao L, et al. Ranking of interventions to reduce dwelling overheating during heat waves. *Energy and Buildings* 2012; 55: 16-27. DOI: http://doi.org/10.1016/j.enbuild.2012.01.043.
49. Gupta R and Gregg M. Preventing the overheating of English suburban homes in a warming climate. *Building Research & Information* 2013; 41: 281-300. DOI: http://doi.org/10.1080/09613218.2013.772043.
50. EEA. Household energy consumption for space heating per m2, https://www.eea.europa.eu/data-and-maps/daviz/unit-consumption-of-space-heating#tab-chart_1 (2014, accessed 10 March 2019).
51. BEIS. National Energy Efficiency Data-Framework (NEED) table creator 2016-csv file. 28 June 2018 ed.: Department for Business, Energy & Industrial Strategy, UK, 2018.
52. Beizaee A, Lomas KJ and Firth SK. National survey of summertime temperatures and overheating risk in English homes. *Building and Environment* 2013; 65: 1-17. DOI: http://doi.org/10.1016/j.buildenv.2013.03.011.
53. CIBSE. CIBSE Weather Data Sets, http://www.cibse.org/knowledge/cibse-other-publications/cibse-weather-data-current,-future,-combined-dsys (2013, accessed 5th May 2014).
54. GLOBE Task Team H, David A., Paula K. Dunbar, Gerald M. Elphingstone, Mark Bootz, Hiroshi Murakami, Hiroshi Maruyama, Hiroshi Masaharu, Peter Holland, John Payne, Nevin A. Bryant, Thomas L. Logan, J.-P. Muller, Gunter Schreier, and John S. MacDonald. The Global Land One-kilometer Base Elevation (GLOBE) Digital Elevation Model, Version 1.0, (1999, accessed 26 March 2019).
55. Cressie NAC. *Statistics for spatial data*. J. Wiley, 1993.

56. Fanchi J. *Integrated reservoir asset management: principles and best practices*. Gulf Professional Publishing, 2010.
57. Crawley DB. Estimating the impacts of climate change and urbanization on building performance. *Journal of Building Performance Simulation* 2008; 1: 91-115. DOI: http://doi.org/10.1080/19401490802182079.
58. Chow DH and Levermore GJ. The effects of future climate change on heating and cooling demands in office buildings in the UK. *Building Services Engineering Research and Technology* 2010; 31: 307-323. DOI: http://doi.org/10.1177/0143624410371284.
59. Ward IC. Will global warming reduce the carbon emissions of the Yorkshire Humber Region's domestic building stock—A scoping study. *Energy and Buildings* 2008; 40: 998-1003. DOI: https://doi.org/10.1016/j.enbuild.2007.08.007.
60. Liu C. Dataset for Current and Future Test Reference Years at a 5km Resolution. University of Bath Research Data Archive, UK2019.
61. IPCC. Emission Scenarios, http://www.ipcc.ch/ipccreports/sres/emission/index.php?idp=0 (2000, accessed 20 September 2015).
62. CIBSE. CIBSE Guide A: Environmental Design. London: The Chartered Institution of Building Services Engineers, 2006.

List of Figures